



## OPEN ACCESS

EDITED BY  
Christian Sohlenkamp,  
National Autonomous University  
of Mexico, Mexico

REVIEWED BY  
Béatrice Roche,  
University of Basel, Switzerland  
Chris Sham,  
National University of Singapore,  
Singapore  
Robson Francisco De Souza,  
University of São Paulo, Brazil

\*CORRESPONDENCE  
Jeff Errington  
jeff.errington@ncl.ac.uk

SPECIALTY SECTION  
This article was submitted to  
Microbial Physiology and Metabolism,  
a section of the journal  
Frontiers in Microbiology

RECEIVED 27 July 2022  
ACCEPTED 22 September 2022  
PUBLISHED 13 October 2022

CITATION  
Kepplinger B, Wen X, Tyler AR,  
Kim B-Y, Brown J, Banks P, Dashti Y,  
Mackenzie ES, Wills C, Kawai Y,  
Waldron KJ, Allenby NEE, Wu LJ,  
Hall MJ and Errington J (2022)  
Mirubactin C rescues the lethal effect  
of cell wall biosynthesis mutations  
in *Bacillus subtilis*.  
*Front. Microbiol.* 13:1004737.  
doi: 10.3389/fmicb.2022.1004737

COPYRIGHT  
© 2022 Kepplinger, Wen, Tyler, Kim,  
Brown, Banks, Dashti, Mackenzie, Wills,  
Kawai, Waldron, Allenby, Wu, Hall and  
Errington. This is an open-access  
article distributed under the terms of  
the [Creative Commons Attribution  
License \(CC BY\)](https://creativecommons.org/licenses/by/4.0/). The use, distribution  
or reproduction in other forums is  
permitted, provided the original  
author(s) and the copyright owner(s)  
are credited and that the original  
publication in this journal is cited, in  
accordance with accepted academic  
practice. No use, distribution or  
reproduction is permitted which does  
not comply with these terms.

# Mirubactin C rescues the lethal effect of cell wall biosynthesis mutations in *Bacillus subtilis*

Bernhard Kepplinger<sup>1</sup>, Xin Wen<sup>2</sup>, Andrew Robert Tyler<sup>2</sup>,  
Byung-Yong Kim<sup>3</sup>, James Brown<sup>1</sup>, Peter Banks<sup>4</sup>,  
Yousef Dashti<sup>1</sup>, Eilidh Sohini Mackenzie<sup>4</sup>, Corinne Wills<sup>2</sup>,  
Yoshikazu Kawai<sup>1</sup>, Kevin John Waldron<sup>4</sup>,  
Nicholas Edward Ellis Allenby<sup>3</sup>, Ling Juan Wu<sup>1</sup>,  
Michael John Hall<sup>2</sup> and Jeff Errington<sup>1,3\*</sup>

<sup>1</sup>Centre for Bacterial Cell Biology, Newcastle University, Newcastle upon Tyne, United Kingdom, <sup>2</sup>Chemistry, School of Natural and Environmental Sciences, Newcastle University, Newcastle upon Tyne, United Kingdom, <sup>3</sup>Odyssey Therapeutics Inc., Newcastle upon Tyne, United Kingdom, <sup>4</sup>Faculty of Medical Sciences, Bioscience Institute, Newcastle University, Newcastle upon Tyne, United Kingdom

Growth of most rod-shaped bacteria is accompanied by the insertion of new peptidoglycan into the cylindrical cell wall. This insertion, which helps maintain and determine the shape of the cell, is guided by a protein machine called the rod complex or elongasome. Although most of the proteins in this complex are essential under normal growth conditions, cell viability can be rescued, for reasons that are not understood, by the presence of a high (mM) Mg<sup>2+</sup> concentration. We screened for natural product compounds that could rescue the growth of mutants affected in rod-complex function. By screening > 2,000 extracts from a diverse collection of actinobacteria, we identified a compound, mirubactin C, related to the known iron siderophore mirubactin A, which rescued growth in the low micromolar range, and this activity was confirmed using synthetic mirubactin C. The compound also displayed toxicity at higher concentrations, and this effect appears related to iron homeostasis. However, several lines of evidence suggest that the mirubactin C rescuing activity is not due simply to iron sequestration. The results support an emerging view that the functions of bacterial siderophores extend well beyond simply iron binding and uptake.

## KEYWORDS

mirubactin, *B. subtilis*, cell wall mutants, siderophore, chemical biological activity

## Introduction

Gram-positive bacteria surround their cell membrane with a thick layer of peptidoglycan (PG), which gives the bacteria their shape and protects them from fluctuations in internal osmotic pressure (Koch, 2006). PG synthesis is highly conserved across bacterial taxa and several components of the PG synthetic machinery are hugely important antibiotic targets. The cell envelopes of Gram-positive bacteria usually contain other highly abundant anionic polymers called teichoic acids (TAs), which can be either anchored into the cell membrane (lipoteichoic acids, LTA) or to the peptidoglycan (wall teichoic acids, WTA) (Archibald et al., 1961). The specific functions of these polymers are not well understood but this certainly includes a role in metal homeostasis (Archibald et al., 1961; Heptinstall et al., 1970) and they can be important virulence determinants in pathogens (Morath et al., 2001; Weidenmaier et al., 2004; Fittipaldi et al., 2008).

Cell wall synthesis is supported by various synthetic systems. In most rod-shaped bacteria cell elongation is governed by various general elements: a “Rod complex,” which includes a glycosyl transferase, RodA, and associated transpeptidases called class B penicillin-binding proteins (bPBPs); autolytic hydrolases such as CwlO and LytE in *Bacillus subtilis* (Masayuki et al., 2012), which break bonds to allow cell wall expansion; and a topological regulator, the actin-like protein MreB, and its associated factors MreC and MreD. Some TA-synthetic enzymes and PG precursor synthetic proteins are also probably associated with the Rod complex (Bhavsar et al., 2001).

In *B. subtilis*, there are three MreB paralogues, which have overlapping functions (Kawai et al., 2009). MreB and Mbl (“MreB-like”) (Levin et al., 1992; Varley and Stewart, 1992; Lee and Price, 1993; Abhayawardhane and Stewart, 1995) are both essential in typical microbiological growth media but, curiously, this growth deficiency can be rescued by addition of high concentrations of magnesium ( $Mg^{2+}$ ) to the culture medium (Formstone and Errington, 2005). Intriguingly, growth of mutants that lack one of several other factors in the Rod complex can also be rescued or greatly enhanced by  $Mg^{2+}$  supplementation, including *mreC*, *mreD* and *rodA* (Jones et al., 2001; Formstone and Errington, 2005; Leaver and Errington, 2005; Dominguez-Cuevas et al., 2012). *B. subtilis*, like most other bacteria, has a second PG synthetic machinery based around bifunctional (glycosyl transferase, transpeptidase) class A penicillin-binding proteins (aPBPs) (Meeske et al., 2016; Emami et al., 2017; Dion et al., 2019). Growth of mutants affected in the major aPBP gene, *ponA*, are also rescued by  $Mg^{2+}$  (Murray et al., 1998). The molecular basis for this  $Mg^{2+}$  effect remains unclear. Formstone and Errington suggested two potential mechanisms: stiffening of

the cell wall or inhibition of autolytic enzymes (Formstone and Errington, 2005; Dajkovic et al., 2017; Tesson et al., 2022). Dajkovic et al. (2017) subsequently presented evidence to exclude mechanical changes in the cell wall, and provided strong evidence for the reduction of autolytic activity. Wilson and Garner (2021) identified LytE as a likely target for this inhibition.

The TAs are underexplored potential antibiotic targets for Gram-positive pathogens. Compounds active on WTA (Campbell et al., 2012) or LTA (Richter et al., 2013; Vickery et al., 2018) have been described but, so far, have not yet entered clinical development. The key enzyme in LTA synthesis, LTA synthase (LtaS), is a particularly interesting antibiotic target because it is essential under normal conditions in *Staphylococcus aureus* (Oku et al., 2009; Corrigan et al., 2011), but specific inhibitors would not affect Gram-negative nor many other Gram-positive bacteria. Furthermore, the enzyme’s active site is located outside the cytoplasmic membrane, excluding cell permeability and efflux mechanisms as sources of resistance. Lastly there is no equivalent in mammalian cells.

We previously described the discovery of mutations in *ltaS* as potent suppressors of the  $Mg^{2+}$ -dependence of *mbl* mutants in *B. subtilis* (Schirner et al., 2009). This suggested that inhibitors of LtaS might also rescue the growth of an *mbl* mutant cultured in the absence of  $Mg^{2+}$ , providing the basis for a powerful chemical biology screen for LtaS inhibitors. Even if compounds rescuing the growth of an *mbl* mutant did not directly target LtaS they might still be of interest by providing insights into the molecular basis for the  $Mg^{2+}$ -rescue effect and the functions of TAs.

Actinomycetes have been a rich source of bioactive natural products including many diverse drugs, particularly antibiotics (Genilloud, 2017). By screening a collection of actinomycete extracts we were able to identify, isolate and characterize a small natural product molecule, mirubactin C (Pu et al., 2022), which efficiently rescues the growth of an *mbl* mutant in the absence of added  $Mg^{2+}$ . We used bioactivity-guided fractionation to purify the molecule and determined its structure by a combination of NMR and high resolution mass spectrometry. The molecule turns out to be identical to a fragment of a known siderophore antibiotic called mirubactin (Giessen et al., 2012; Kishimoto et al., 2015b). To validate the source of the observed bioactivity, mirubactin C was synthesized, and the synthetic molecule was also able to rescue growth of *mbl* and *mreB* mutants of *B. subtilis* but was toxic at higher concentrations, probably due to iron sequestration. The results provide new insights into the intricate connections between metal homeostasis and cell envelope synthesis systems, as well as highlighting how poorly we understand the complex chemical exchanges between microorganisms inhabiting the soil.

## Results

### A screen for natural product compounds that rescue growth of an *mbl* mutant

Previous results showed that disruption of the *mbl* gene is normally lethal on standard culture media but that the mutant can be rescued by the addition of a high concentration (e.g., 20 mM) of  $Mg^{2+}$ . Cells of the *mbl* mutant cultured in the presence of  $Mg^{2+}$  and then diluted into medium with no added  $Mg^{2+}$  failed to grow, except after prolonged incubation, at which time it appeared that suppressor mutations emerged that relieve the  $Mg^{2+}$  dependence, as described by Schirner et al. (2009). We established a protocol for culturing *mbl*-mutant cells in 96 well plates. **Supplementary Figure 1** shows that, under these conditions, addition of 20 mM  $Mg^{2+}$  resulted in growth albeit slower than that of isogenic wild type cells (*B. subtilis* 168CA). Lower concentrations of  $Mg^{2+}$  (down to 5 mM) allowed equivalent growth rates but with an increasingly long delay. We do not understand the basis of this but a similar effect has been described by Pi et al. (2022). Agar plate crush extracts (see Materials and methods) of strains from a large collection of actinomycetes that is both diverse and low in replicate organisms were obtained from Demuris Ltd. A total of 2,070 extracts were screened, from organisms belonging to many Genera, including: *Actinomadura*, *Amycolatopsis*, *Dactylosporangium*, *Gordonia*, *Micromonospora*, *Nocardia*, *Rhodococcus*, *Streptacidiphilus*, *Streptomyces* and *Streptosporangium*. The collection is known to contain a high proportion of antibiotic producers, with about 25% of organisms capable of producing secondary metabolites that kill *B. subtilis* in simple plug assays. Five of the strain extracts were found reproducibly to enhance the growth of the *mbl* mutant in the absence of added  $Mg^{2+}$ , giving growth rates similar to 5–10 mM of  $Mg^{2+}$  (representative plots shown in **Supplementary Figure 1**).

### Genome sequencing of the producer strains

To facilitate purification of the active compounds we tested the supernatants of the five positive strains for the *mbl*-rescuing activity. Of the five strains, only TW 167, MEX267 and MDA8-470 produced *mbl*-rescuing activity under these conditions, so we focused on these three strains. As a method to determine what kind of bioactive natural products these organisms might make and whether they were likely to make similar or different compounds, we carried out whole genome sequencing (WGS) by a combination of Minion and Illumina sequencing methods (NCBI accession numbers: JANADG0000000000 TW 167, CP098740 MDA8-470,

JANADF0000000000 Mex267). Analyses of the predicted natural product biosynthetic gene clusters in each of the three strains are shown in **Supplementary Table 1** through antiSMASH output of the prioritized strains. This analysis revealed that TW 167 and MDA8-470 are closely related strains, whereas MEX267 is evolutionarily distant. The nearest described type strains were *Streptomyces drozdowiczii* for TW 167 and MDA8-470 and *Nocardia zapadnayensis* for MEX267. We chose MDA8-470 as the focus of further work since in repeated growth experiments it tended to provide bioactivity more consistently than the other strains.

### Purification and structure determination of the active compound from MDA8-470

We purified the active component from supernatants of strain MDA8-470 by activity-guided isolation using the *mbl*-rescue bioassay. MDA8-470 was cultured for 76.5 h at 26 L volume in a stirred tank reactor. The culture broth was treated with XAD-16 resin and absorbed compounds were eluted with methanol. Hydrophobic compounds were removed by partitioning between ethyl acetate (EtOAc) and water (pH 4). The active compound stayed in the aqueous phase which was further purified by C18 flash chromatography followed by LH20 size exclusion in water and then freeze dried to give a light brown powder with a molecular ion by high resolution mass spectrometry (HRMS) of  $m/z$  427.1815  $[M + H]^+$ .

### Mirubactin C is a fragment of the siderophore antibiotic mirubactin A

The molecular structure of the active compound was determined by a combination of HRMS and NMR spectroscopy (**Supplementary Table 3** and **Supplementary Figure 2**). HRMS suggested a molecular formula of  $C_{18}H_{25}O_8N_4$ , implying eight double bond equivalents in the structure.  $^1H$  NMR in  $D_2O$  allowed the identification of 18 hydrogens, suggesting the presence of 7 exchangeable protons, whilst  $^{13}C$  NMR showed the presence of a benzene ring and four carbonyl-containing functional groups. Further analysis by  $^{15}N$  NMR confirmed the presence of four nitrogen atoms, one amine and three amide-like groups. This, combined with additional 2D experiments, allowed us to propose a linear polypeptide-like structure, including both a 2,3-dihydroxybenzoyl and a hydroxamic acid group typical of bacterial siderophores (**Figure 1**).

The structure of the compound turned out to be identical to a recently described compound, Mirubactin C (Pu et al., 2022), which belongs to a family of related compounds including

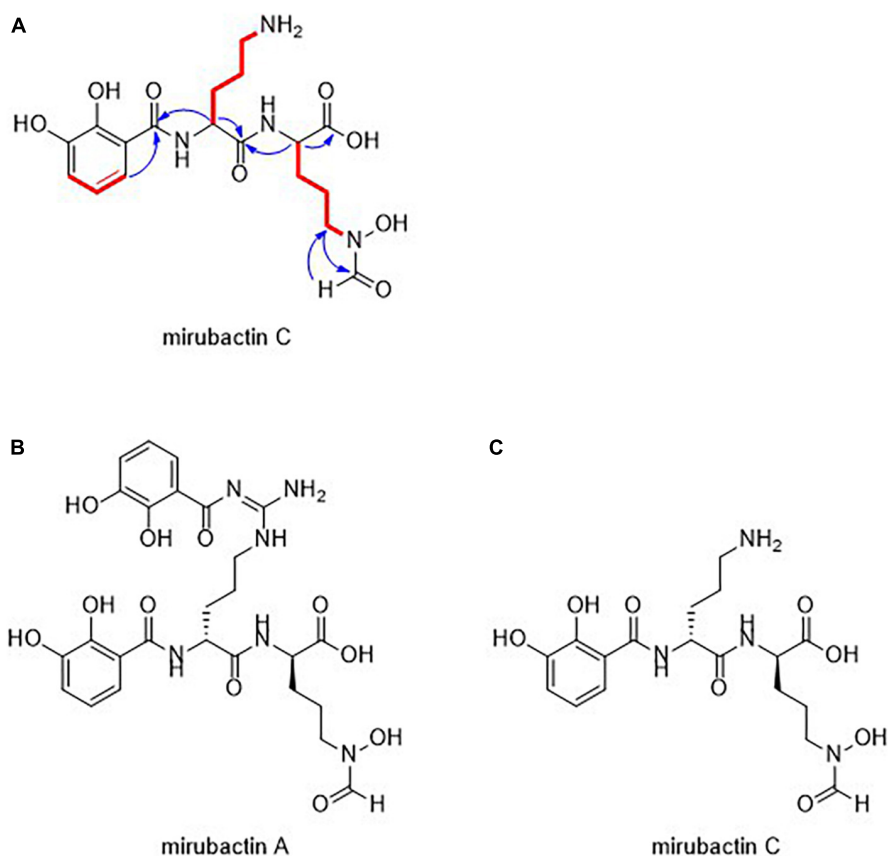


FIGURE 1

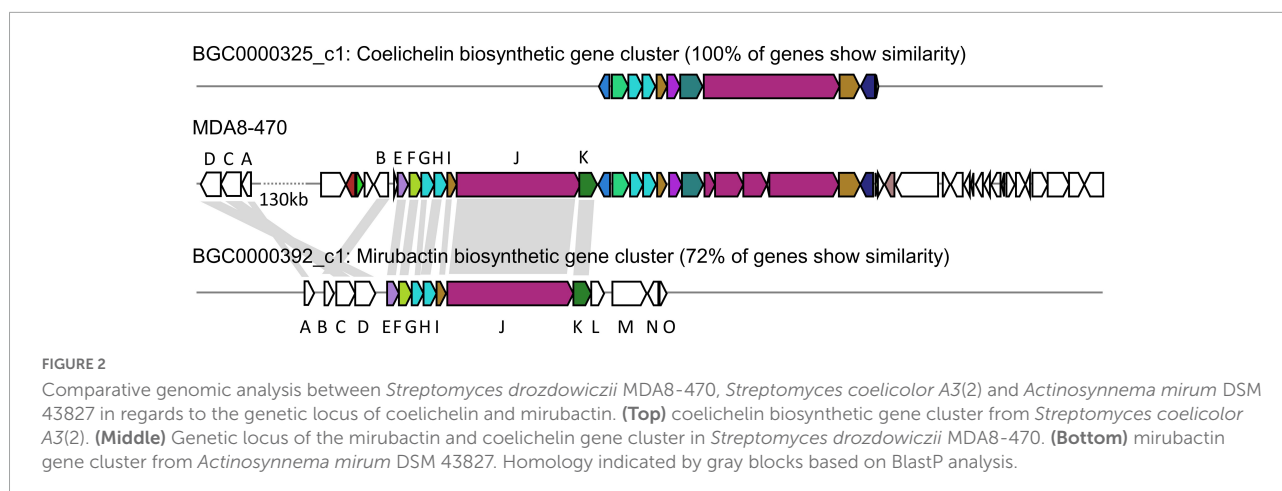
(A) Structural assignment of mirubactin C (COSY = red, selected HMBC = blue) (B) Structures of mirubactin A (C) mirubactin C.

mirubactin A, chlorocatechelin A and chlorocatechelin B. Mirubactin C is identical to mirubactin A, except that it is missing one of its 2,3-dihydroxybenzoid acid moieties and has lost the guanidine group. The relationship between mirubactin A and mirubactin C is similar to that of chlorocatechelin A to B (Kishimoto et al., 2014). Indeed, mirubactin C differs from chlorocatechelin B only in the lack of a chlorine substituent on the aromatic ring. Kishimoto et al. (2014, 2015a) proposed that chlorocatechelin A spontaneously decomposes to give chlorocatechelin B under acidic conditions, (Kishimoto et al., 2014, 2015a) raising the possibility that mirubactin C has a similar relationship as a degradation product of mirubactin A (Supplementary Figure 4). This was recently shown by Pu et al. (2022). To check whether mirubactin A was produced by MAD8-470, the strain was cultured in 50 ml of GYM media for 3 days and, after removing the bacterial cells, the chemical profile of culture media was directly analysed by LC-MS. Mirubactin A was detected in both apo ( $m/z$  605.2) and holo ( $m/z$  658.1) forms (Giessen et al., 2012).

Marfy's analysis was used to determine the stereochemistry of the two constituent ornithine amino acid moieties, which were both found to be in the D-form, matching

those of mirubactin A and the chlorocatechelins (Supplementary Figure 3).

We identified a mirubactin-like gene cluster in the genome sequence of MDA8-470 by a combination of antiSMASH analysis and alignments with the mirubactin A gene cluster from *Actinosynnema mirum* DSM 43827 (Figure 2 and Supplementary Figure 2). The gene cluster borders on the gene cluster of coelichelin (an unrelated siderophore) and is consequently not immediately identified as mirubactin by antiSMASH. However, the subcluster analysis found the mirubactin gene cluster with an identity of 72%. The gene cluster appears to be truncated on both sides, while the core biosynthetic pathway is conserved. The biosynthetic genes [*mrBA*, *mrBC* and *mrBD*; gene designations as assigned by Giessen et al. (2012)] for the 2,3-dihydroxybenzoic acid groups (DHAB) appear to be missing from the main cluster. However, genes sharing homology with *mrBC* (57%), *mrBA* (56%) and *mrBD* (55%) were found in an operon approximately 130 kb upstream of the gene cluster. Genes *mrBL*-*mrBO* appear to be missing in MDA8-470 but they were annotated as unknown function and regulatory in the original mirubactin cluster, and therefore may not be required for the synthesis of mirubactin A.



## Synthetic mirubactin C rescues growth of the *mbl* mutant

To confirm that mirubactin C was responsible for the rescue of *mbl* mutant growth we undertook a total synthesis of the compound and compared the activity of this synthetic material to the natural product. Synthetic mirubactin C rescued growth at the same concentration as the purified natural compound (Figures 3A,B). We therefore conclude that the structure shown in Figure 1 (mirubactin C) is indeed the compound responsible for the *mbl*-growth-rescue effect in extracts from strain MDA8-470. Detailed dose response curves for rescue by the compound (also observed with the original culture extracts) revealed an optimal rescue concentration at 4  $\mu\text{g/ml}$ : above this concentration, growth rescue was progressively less effective (Figure 3A). To ascertain how specific this effect is we also purified mirubactin A and tested it in the *mbl*-recovery assay (Figure 3C). Mirubactin A only showed slight rescue of the *mbl* mutant and required 8 times the concentration (32  $\mu\text{g/ml}$  vs 4  $\mu\text{g/ml}$ ). A concentration of 32  $\mu\text{g/ml}$  of mirubactin C already had an adverse effect on the growth of the *mbl* mutant. The failure to rescue growth of the *mbl* mutant at higher concentrations of mirubactin C appeared to be an inhibitory activity, as growth of wild type *B. subtilis* was also impaired at the higher concentrations (Figure 3D). Addition of the optimal concentration of mirubactin C not only rescued growth of the *mbl* mutant, it also largely restored a normal cell morphology, although the cells seemed more prone to chaining than normal (Figure 4).

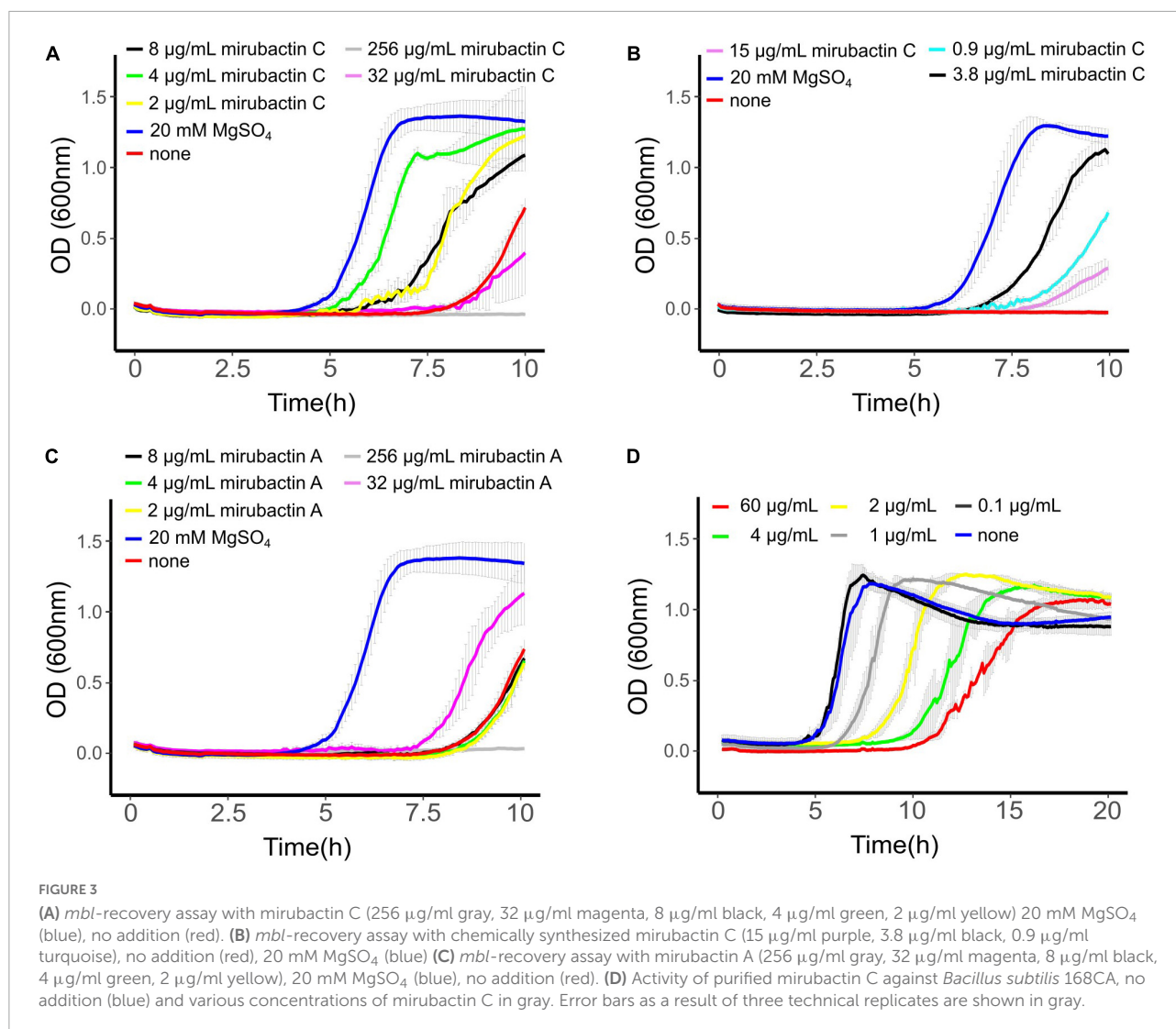
## Mirubactin C also rescues the growth of MreB but not aPBP mutants

Previous work has revealed that various mutations affecting PG synthesis are lethal under “normal” culture conditions but can be rescued by addition of high concentrations of  $\text{Mg}^{2+}$ ,

including *mreB*, *mreC*, *mreD*, *rodA* and *ponA*, and that this is likely due to the inhibition of PG hydrolases (see above). We therefore tested whether mirubactin C could rescue other mutants with a  $\text{Mg}^{2+}$ -dependent phenotype. As shown in Figure 4, mirubactin C rescued the growth of the  $\Delta\text{mreB}$  mutant, but not that of the  $\Delta 4$  mutant (which lacks *ponA* and the 3 other class A PBPs) (Emami et al., 2017). Although growth of the  $\Delta\text{mreB}$  mutant was restored, the cells were highly abnormal morphologically, being bloated and lytic (Figure 4).

## The inhibitory effect of mirubactin C is associated with iron homeostasis

The mechanism whereby mirubactin C rescues growth of the *mbl* and *mreB* mutants was not clear but we reasoned that a clue might come from further investigation of the inhibitory effect. As one way to investigate this we took a library of *B. subtilis* deletion mutants (Koo et al., 2017) and tested the set for growth at a subinhibitory concentration of mirubactin C. Three genes *odhA*, *odhB* and *gpsA* (enzymes involved in the TCA cycle and biosynthesis of phospholipids) grew better in the presence of mirubactin C (Supplementary Figure 5). The nine most severely affected mutants are listed in Table 1 and the full data set is provided in Supplementary Figure 5. Interestingly five of the nine genes are involved in iron (Fe) homeostasis. These findings suggested that mirubactin C binds iron and that at concentrations above 4  $\mu\text{g/ml}$ , under the conditions used, it causes iron limitation resulting in growth inhibition. To test this idea, we determined the Fe and  $\text{Mg}^{2+}$  content of wild type and mutant *B. subtilis* cells by inductively coupled plasma mass spectrometry (ICP-MS) (Figure 5) after culture in the presence of  $\text{Mg}^{2+}$  or mirubactin C. We observed that cells treated with mirubactin C contained significantly lower  $\text{Mg}^{2+}$  and Fe content. Interestingly, growth-restoring concentrations of mirubactin C did not rectify the  $\text{Mg}^{2+}$  deficiency of *mreB* or *mbl* cells, confirming that the



metabolite restores their growth through a mechanism distinct from that of  $\text{Mg}^{2+}$  (Figure 5). To confirm the role of Fe, we incubated wild type *B. subtilis* with an inhibitory concentration of mirubactin C (60  $\mu\text{g}/\text{mL}$ ) and supplemented the culture with  $\text{FeCl}_3$ . As shown in Figure 6, growth was partially restored at 3  $\mu\text{M}$   $\text{Fe}^{3+}$  and fully restored at 50  $\mu\text{M}$ . This indicates that toxicity of mirubactin C at concentrations above 4  $\mu\text{g}/\text{mL}$  is likely due to Fe starvation, consistent with the idea that this compound, like its larger relative mirubactin A, binds iron.

## Discussion

The main motivation for developing our chemical biology screen was to find potential inhibitors of the LtaS protein, a potential antibiotic target, given that Schirmer et al. (2009) had shown that deletion of the *ltaS* gene rescues growth of

*mbl* mutants. However, since Schirmer et al. (2009) found suppressor mutations in several other genes, the screen might also identify compounds acting on other targets. Further studies of the hit compounds might also provide insights into the enigmatic ability of  $\text{Mg}^{2+}$  to rescue the growth of mutants affected in various other cell wall functions. In this work we only screened about 2,000 natural product extracts but this unearthed mirubactin C, plus at least one other structurally and functionally distinct compound that awaits further investigation. It is likely that a screen of larger numbers of extracts would yield yet more interesting compounds, including potential antibiotics. Thus, further screening of synthetic or natural compounds via the *mbl*-rescue assay is warranted.

One of the historical difficulties with screens of natural product compounds was that of dereplicating the hits, i.e., identifying strains likely to be making the same compound and therefore reducing the number of active strains to study via

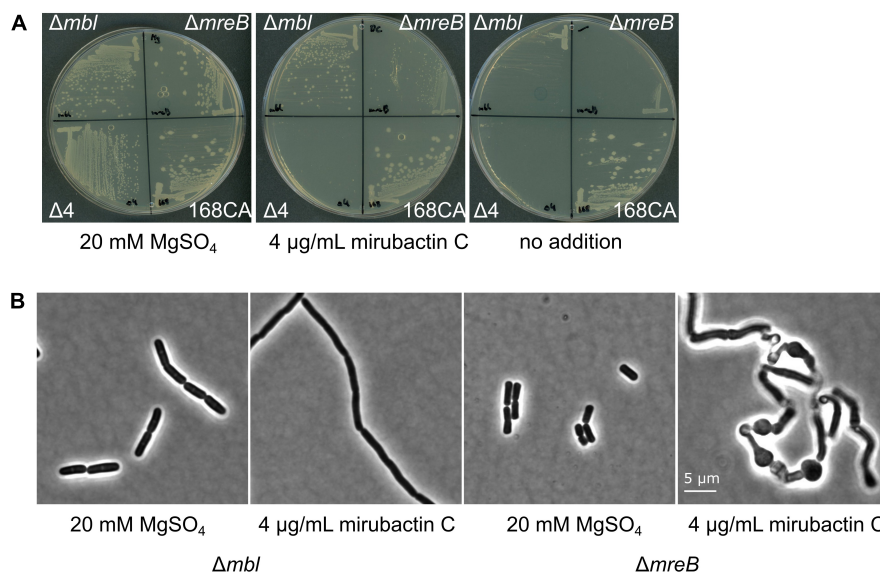


**FIGURE 4**  
 Effects of divalent cations and mirubactin C on several  $MgSO_4$ -dependent cell wall mutants. **(A)** Growth behavior of *Bacillus subtilis* 168CA (wt) and  $\Delta mbl$ ,  $\Delta mreB$ ,  $\Delta 4$  mutant (which lacks *ponA* and genes for the 3 other class A PBPs) on PAB plates in the presence of 20 mM  $MgSO_4$ , 4  $\mu g/ml$  mirubactin C and in the absence of any additive. **(B)** Phenotype of *Bacillus subtilis* mutants  $\Delta mbl$  and  $\Delta mreB$  in the presence of  $MgSO_4$  and 4  $\mu g/ml$  mirubactin C.

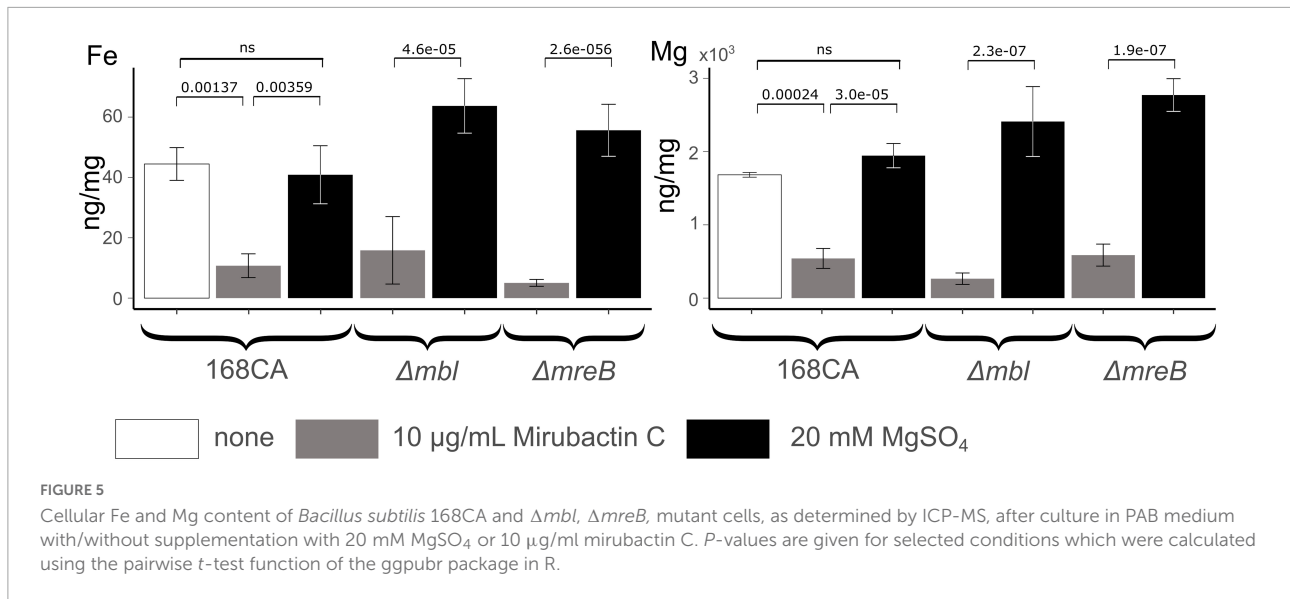
**TABLE 1** Deletion strains that exhibit hypersensitivity to mirubactin C.

Gene	Proposed function according to Subtiwiki (Pedreira et al., 2022)
<i>feuA</i>	ABC transporter for the siderophores Fe-enterobactin and Fe-bacillibactin (binding protein), with YusV as ATPase
<i>yusV</i>	ABC transporter for the siderophores Fe-enterobactin and Fe-bacillibactin, as well as for the siderophores schizokinen and arthrobactin (ATPase)
<i>cpgA</i>	Ribosome assembly GTPase, activity stimulated by ribosomes, may be involved in the maturation of the 30S subunit of the ribosome, detoxification of 4-phosphoerythronate
<i>yqhY</i>	Modulator of lipid biosynthesis
<i>feuB</i>	ABC transporter for the siderophores Fe-enterobactin and Fe-bacillibactin (integral membrane protein)
<i>feuC</i>	ABC transporter for the siderophores Fe-enterobactin and Fe-bacillibactin (integral membrane protein)
<i>flhA</i>	Part of the flagellar type III export apparatus (flagellar Type III secretion system), part of the CORE complex required for flagellum and nanotube assembly
<i>fur</i>	Transcription regulator of iron homeostasis, sensor of Fe sufficiency
<i>sdhA</i>	Succinate dehydrogenase (flavoprotein subunit)

culture scale-up and compound purification. Rapid WGS of the three main hits revealed that two strains were almost identical and therefore likely to be making the same active compound. It was therefore only necessary to follow up one of these strains, illustrating the power of the genomic dereplication approach. The sequencing and analysis also revealed that the third strain is very different to the others and therefore is likely to make an unrelated compound. We intend to follow this up in the future.

The purified active compound turned out to be a smaller version of a known siderophore antibiotic, mirubactin. Total synthesis of the structure deduced for mirubactin C confirmed that this is the active compound in extracts of the producer strain. The genome sequence suggests that strain MDA8-470 contains all necessary genes for biosynthesis of mirubactin

and metabolic profile of culture media of strain MDA8-470 confirmed production of mirubactin. Thus, it seems likely that mirubactin C is either a shunt metabolite in the biosynthesis of mirubactin a or a breakdown product of mirubactin A (Supplementary Figure 4), which would mirror the findings of Kishimoto et al. (2014) with the related chlorocatechelin A and B compounds. Mirubactin A has a high affinity for  $Fe^{3+}$  due to its hexadentate coordination potential based on its DHBA (x2) and hydroxamate moieties. Mirubactin C has a lower affinity for  $Fe^{3+}$  because of the absence of one of the DHBA groups (Pu et al., 2022). However, mirubactin C is clearly capable of binding Fe because: first, the inhibitory effect we saw in cultures treated with  $\geq 16 \mu g/ml$  mirubactin C was exacerbated by various mutations affected in iron uptake



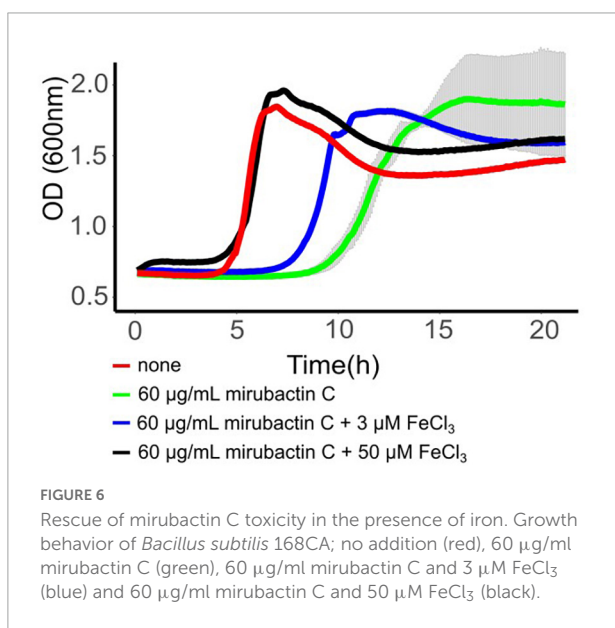
or homeostasis; second, the inhibitory effect was alleviated by Fe supplementation in the growth medium. Nevertheless, the rescuing effect of mirubactin C at low Fe concentrations is not simply due to it acting to import iron because mirubactin A hardly rescued the *mbl* mutant. Furthermore, although most actinomycete bacteria produce iron siderophores, only a tiny proportion of the > 2,000 culture extracts we tested rescued growth of the mutant. One mechanistic hypothesis worthy of future testing is that mirubactin C moderates siderophore transport in *Bacillus*. This could occur by affecting import through the FeuABC siderophore transporter, in which the FeuA component is known to exhibit promiscuous siderophore binding (Peuckert et al., 2011), by interfering with *feuABC*

regulation by interacting with its regulator Btr, which contains a FeuA-like sensory domain (Gaballa and Helmann, 2007), or by modifying the activity of the siderophore esterase, BesA (Miethke et al., 2006). Further work will be needed to establish the mechanism whereby mirubactin C rescues growth of the Rod complex mutants. The finding of a natural product compound that has a growth restorative effect on mutants of the Rod pathway highlights that there is much still to be learned about the complex chemical genetic interactions between soil microbes.

## Materials and methods

### Development of a robust high throughput assay for rescue of *mbl*-mutant growth

The *mbl* mutant was cultured in nutrient broth (NB) containing 20 mM  $Mg^{2+}$  under defined conditions and then diluted  $10^{-4}$ -fold into fresh medium containing no added  $Mg^{2+}$  and chloramphenicol or spectinomycin (to inhibit growth of the actinomycetes; see below). The mutant culture was dispensed into the wells of a 96 well microtiter plate containing various controls and test samples. To calibrate the assay, several defined concentrations of  $Mg^{2+}$  were included. The plates were cultured at 37°C for 15 h, and growth was monitored by following the optical density ( $OD_{600}$ ). A wild type culture was also included, with no added  $Mg^{2+}$ . No growth of the *mbl* mutant was seen in the absence of  $Mg^{2+}$  but addition of different concentrations of  $Mg^{2+}$  resulted in growth after a delay, which was roughly proportional to the amount of  $Mg^{2+}$  added. A typical result is shown below (Supplementary Figure 1), with time (min) along



the x-axis and optical density (OD<sub>600</sub>) on the y-axis. Remaining wells in the plate were occupied by test extracts from the Demuris actinomycete collection. After testing various methods, a freeze-thaw-centrifuge procedure was adopted for preparation of extracts. Individual actinomycete strains were cultured on an appropriate agar growth medium. The agar was harvested and fragmented into 50 ml conical tubes, which were frozen at  $-20^{\circ}\text{C}$  overnight, then thawed and centrifuged. The supernatant was collected, filtered and stored at  $-20^{\circ}\text{C}$  until used. Positives in the primary assay were identified by growth stimulation similar to  $\text{Mg}^{2+}$  addition. Candidate extracts were retested using new extracts prepared via regrowth of the actinomycete strains. Five positive producers were identified, strains TW 167, A51P1, Mex267, MDA8-470 and MDA8-566.

## Genome sequencing and analyses

The strains TW 167 and MEX267 were grown in 10 ml of liquid GYM and incubated for 3 days at  $30^{\circ}\text{C}$  and 120 rpm. Genomic DNA was extracted using the Quick-DNA HMW MagBead Kit (Zymo Research, cat. no. D6060). Aliquots (300  $\mu\text{l}$ ) of the cultured cells were spun at  $13,000 \times g$  for 2 min to pellet. The cells were resuspended in 200  $\mu\text{l}$  DNA/RNA Shield (Zymo Research, cat. no. R1100-50). Microbial lysis and DNA extraction (including RNase treatment) were performed according to the manufacturer's instructions. DNA quality was assessed by agarose gel electrophoresis to ensure no trace amounts of RNA. DNA concentration was assessed using the dsDNA assay on a Qubit fluorometer.

The strains TW 167 and MEX267 were part of a multiplexed nanopore MinION sequencing (12 strains in total) using the Native Barcoding Expansion 1–12 (EXP-NDB104), in conjunction with the Ligation Sequencing Kit (SQK-LSK109). A DNA fragmentation step was not performed. Priming and loading the SpotON flow cell was performed according to the manufacturer's instructions using R9.4.1 flow cells (FLO-MIN106D, ONT). The flow cell was mounted on a MinION Mk1B device (ONT) for sequencing and was controlled using Oxford Nanopore Technologies MinKNOW software. Base calling and data conversion was performed in parallel using Albacore v1.2.4 (Oxford Nanopore Technologies). The sequences were exported in FASTQ format and used for an assembly with CANU v1.5 (Koren et al., 2017).

For the Illumina Sequencing the genomic DNA libraries were prepared using the Nextera XT Library Prep Kit (Illumina, San Diego, USA) following the manufacturer's protocol with the following modifications: input DNA was increased 2-fold, and PCR elongation time was increased to 45 s. DNA quantification and library preparation were carried out on a Hamilton Microlab STAR automated liquid handling system (Hamilton Bonaduz AG, Switzerland). Pooled libraries were quantified using the Kapa Biosystems Library Quantification Kit for

Illumina. Libraries were sequenced using Illumina sequencers (HiSeq/NovaSeq) using a 250 bp paired-end protocol.

The resulting reads were mapped onto the contigs produced by Canu using Minimap and the resulting consensus sequences exported. The contigs were annotated using Prokka 1.11 (Seemann, 2014). The corrected genome sequences were analysed with the online version of antiSMASH 6.0.1 (Blin et al., 2021).

MDA8-470 was sequenced using the Pacific Biosciences single-molecule, real-time DNA sequencing technology performed by the University of Maryland School of Medicine Genomics Resource Centre who also assembled the genome. The resulting four contigs were further polished using paired-end Illumina MiSeq data and annotated using RAST (Aziz et al., 2008).

## Purification of mirubactin C

The *Streptomyces* isolate MDA8-470 was grown in GYM medium (4 g/L glucose, 4 g/L yeast extract, 10 g/L malt extract) for 76.5h (30 degrees) in two stirred tank bioreactors at a combined volume of 26 L. The combined culture supernatant was subjected to a batch absorption of 1.5 kg Amberlite XAD-16N resin. The resin was eluted with 2.5 L of methanol and evaporated to yield in 900 ml of aqueous extract. The extract was twice extracted at pH 4 with an equal volume of ethyl acetate. Bioactivity-guided fractionation showed that the compound stayed in the aqueous phase. We therefore subjected the active aqueous extract in five batches of about 180 ml to 60 g reverse phase flash chromatography from water (0.1% formic acid) to methanol (0.1% formic acid) (Gradient 1 column volume (CV) water, 10 CV 0–20% methanol, 2 CV 20–100% methanol, 1.5 CV 100% methanol). Mirubactin C eluted at about 10% methanol. The active fractions were combined and freeze-dried to a viscous oil of 5 ml. To remove the formic acid and other minor components we finally subjected the semi pure mirubactin C to a LH20 size exclusion column (85 cm x 3 cm) at a flow rate of 1 ml/min. The active fractions were freeze-dried to give a light brown powder.

## Purification of mirubactin A

A mirubactin producing strain *Streptomyces sanglieri* 2161 (from the Demuris library) was cultured in 1 L GYM media for 3 days. The culture was centrifuged and the supernatant was filtered to remove the cells. The filtrate was passed through a Hypersep C18 (10 g) column using a vacuum pump. The column was then eluted stepwise with 100/0, 90/10, 50/50 and 0/100 of water/methanol. LC-MS analysis showed that mirubactin A eluted in the fraction with 10% methanol. The compound was then further purified on an Agilent 1260 Infinity II preparative HPLC connected to a single-Q mass

spectrometer using the following HPLC method: initial isocratic conditions of 5% acetonitrile for 5 min followed by linear gradient from 5 to 50% acetonitrile over 45 min; then to 100% acetonitrile in 1 min; continued by isocratic flow for an additional 9 min at a flow rate of 12 ml/min. To avoid degradation of mirubactin during chromatography, solvents without acid additives were used. A molecular formula of  $C_{26}H_{32}N_6O_{11}$ , consistent with mirubactin A, was generated for the purified compound based on HRESIMS  $m/z$  605.2198  $[M + H]^+$  (calculated for  $C_{26}H_{33}N_6O_{11}^+$ , 605.2201).

## Bacillus subtilis deletion strain library

The strains from a comprehensive *B. subtilis* deletion library (Koo et al., 2017) were transferred onto agar plates containing LB-Miller agar either with or without 200  $\mu$ g/ml mirubactin C using a SINGER ROTOR colony pinning robot with 384 long pin pads. The agar plates were incubated overnight at 37°C before being imaged on an S&P robotics SP Imager. The IRIS programme (Kritikos et al., 2017) was used to analyse the agar plate photos and determine individual colony size and the mean of four independent pinning experiments was plotted in [Supplementary Figure 5](#).

## Effect of mirubactin C on the growth of *Bacillus subtilis* 168CA, $\Delta mbl$ , $\Delta mreB$ and $\Delta ponA$

*Bacillus subtilis* wild type 168CA, and isogenic strains bearing mutations  $\Delta mbl$ ,  $\Delta mreB$  and  $\Delta ponA$  were grown on nutrient agar plates overnight in the presence of 20 mM  $Mg^{2+}$ . Single colonies of each strain were inoculated into 10 ml PAB medium and grown to an  $OD_{600nm}$  of  $\sim 0.1$ , before diluting  $10^{-4}$  into PAB (Difco Antibiotic Medium 3) containing no  $Mg^{2+}$ . Mirubactin C was dissolved to 10 mg/ml in water prior to making dilutions in PAB medium to reach the final concentrations shown.  $FeCl_3$  was dissolved in water to a concentration of 100 mM prior to making dilutions in PAB to reach the final concentrations. Growth was monitored in 96 well microtiter plate. For microscopy analysis the strain was grown to mid logarithmic phase in a 96 well plate prior to microscopic analysis. Microscopy was carried out with Nikon Eclipse Ti (Nikon Plan Apo 1.40 Oil Ph3 objective) and the images were acquired with a Prime 4.2 sCMOS camera (Photometrics) and Metamorph 7 (Molecular Devices).

## Elemental analysis of *Bacillus subtilis* cells

Overnight cultures of *B. subtilis* strains grown in 10 ml of PAB medium (Difco Antibiotic Medium 3) supplemented

with 20 mM  $Mg^{2+}$ . The cultures were washed twice with magnesium free medium (equal volume), diluted 1:1000 and subsequently cultured in PAB medium (37 degrees), supplemented with 20 mM  $Mg^{2+}$  or with 10  $\mu$ g/ml mirubactin C, to  $OD_{600nm} \sim 0.6$  (in biological triplicates). Cells were harvested by centrifugation and washed in 1 ml of 20 mM HEPES buffer, pH 7.4, followed by a wash in 20 mM EDTA to remove surface-associated metals, then finally washed twice in PBS to remove trace EDTA. The wet cell weight of the samples was determined and then the pellets were digested in 440  $\mu$ l concentrated nitric acid before 10-fold dilution for elemental analysis. ICP-MS analysis was performed by Durham University Bio-ICP-MS Facility using a set of matrix-matched standard solutions containing defined concentrations of  $Mg^{2+}$  and Fe, using Sc and Bi as internal standards in all samples and standards. The p-values were calculated using the pairwise *t*-test function in the ggpubr package in R.

## Data availability statement

The datasets presented in this study can be found in online repositories. The names of the repository/repositories and accession number(s) can be found in the article/[Supplementary material](#).

## Author contributions

BK: investigation, visualization, and writing – original draft. YD, XW, AT, PB, JB, EM, and B-YK: investigation. CW and NA: supervision. YK: conceptualization and writing – review and editing. LW and KW: supervision and writing – review and editing. NA and MH: writing-original draft and supervision. JE: conceptualization, writing – original draft, review and editing, supervision, project administration, and funding acquisition. All authors contributed to the article and approved the submitted version.

## Funding

Work in the JE lab was supported by a BBSRC Follow-on Fund grant (BB/FOF/319) and a Wellcome Investigator Award (209500).

## Acknowledgments

We thank Newcastle University for Ph.D. studentships, Dr. Alex Charlton (SAGE Mass Spectrometry Facility, Newcastle

University) for mass spectrometry support, Prof. William McFarlane (Newcastle University) for NMR support, and Dr. Richard Daniel for the use of the *Bacillus subtilis* knock out library.

## Conflict of interest

NA and B-YK were an employee of and JE scientific founder of and shareholder in Demuris Ltd. (now Odyssey Therapeutics Inc.).

The remaining authors declare that the research was conducted in the absence of any commercial or financial relationships that could be construed as a potential conflict of interest.

## References

- Abhayawardhane, Y., and Stewart, G. C. (1995). *Bacillus subtilis* possesses a second determinant with extensive sequence similarity to the *Escherichia coli* mreB morphogene. *J. Bacteriol.* 177, 765–773. doi: 10.1128/jb.177.3.765-773.1995
- Archibald, A. R., Armstrong, J. J., Baddiley, J., and Hay, J. B. (1961). Teichoic acids and the structure of *Bacterial* walls. *Nature* 191, 570–572. doi: 10.1038/191570a0
- Aziz, R. K., Bartels, D., Best, A. A., DeJongh, M., Disz, T., Edwards, R. A., et al. (2008). The RAST server: rapid annotations using subsystems technology. *BMC Genom.* 9:75. doi: 10.1186/1471-2164-9-75
- Bhavsar, A. P., Beveridge, J. T., and Brown, D. E. (2001). Precise deletion of tagD and controlled depletion of its product, glycerol 3-phosphate cytidylyltransferase, leads to irregular morphology and lysis of *Bacillus subtilis* grown at physiological temperature. *J. Bacteriol.* 183, 6688–6693. doi: 10.1128/JB.183.22.6688-6693.2001
- Blin, K., Shaw, S., Kloosterman, A. M., Charlop-Powers, Z., van Wezel, G. P., Medema, M. H., et al. (2021). antiSMASH 6.0: improving cluster detection and comparison capabilities. *Nucleic Acids Res.* 49:W29–W35. doi: 10.1093/nar/gkab335
- Campbell, J., Singh, A. K., Swoboda, G. J., Gilmore, M. S., Wilkinson, J. B., and Walker, S. (2012). An antibiotic that inhibits a late step in wall teichoic acid biosynthesis induces the cell wall stress stimulon in *Staphylococcus aureus*. *Antimicrob. Agents Chemother.* 56, 1810–1820. doi: 10.1128/AAC.05938-11
- Corrigan, R. M., Abbott, J. C., Burhenne, H., Kaefer, V., and Gründling, A. (2011). c-di-AMP is a new second messenger in *Staphylococcus aureus* with a role in controlling cell size and envelope stress. *PLoS Pathog.* 7:e1002217. doi: 10.1371/journal.ppat.1002217
- Dajkovic, A., Tesson, B., Chauhan, S., Courtin, P., Keary, R., Flores, P., et al. (2017). Hydrolysis of peptidoglycan is modulated by amidation of meso-diaminopimelic acid and Mg<sup>2+</sup> in *Bacillus subtilis*. *Mol. Microbiol.* 104, 972–988. doi: 10.1111/mmi.13673
- Dion, M. F., Kapoor, M., Sun, Y., Wilson, S., Ryan, J., Vigouroux, A., et al. (2019). *Bacillus subtilis* cell diameter is determined by the opposing actions of two distinct cell wall synthetic systems. *Nat. Microbiol.* 4, 1294–1305. doi: 10.1038/s41564-019-0439-0
- Dominguez-Cuevas, P., Mercier, R., Leaver, M., Kawai, Y., and Errington, J. (2012). The rod to L-form transition of *Bacillus subtilis* is limited by a requirement for the protoplast to escape from the cell wall sacculus. *Mol. Microbiol.* 83, 52–66. doi: 10.1111/j.1365-2958.2011.07920.x
- Emami, K., Guyet, A., Kawai, Y., Devi, J., Wu, L. J., Allenby, N., et al. (2017). RodA as the missing glycosyltransferase in *Bacillus subtilis* and antibiotic discovery for the peptidoglycan polymerase pathway. *Nat. Microbiol.* 2:16253. doi: 10.1038/nmicrbiol.2016.253
- Fittipaldi, N., Sekizaki, T., Takamatsu, D., Harel, J., Dominguez-Punaro, M., de la, C., et al. (2008). D-alanylation of lipoteichoic acid contributes to the virulence of *Streptococcus suis*. *Infect. Immun.* 76, 3587–3594. doi: 10.1128/IAI.01568-07
- Formstone, A., and Errington, J. (2005). A magnesium-dependent mreB null mutant: implications for the role of mreB in *Bacillus subtilis*. *Mol. Microbiol.* 55, 1646–1657. doi: 10.1111/j.1365-2958.2005.04506.x
- Gaballa, A., and Helmann, J. D. (2007). Substrate induction of siderophore transport in *Bacillus subtilis* mediated by a novel one-component regulator. *Mol. Microbiol.* 66, 164–173. doi: 10.1111/j.1365-2958.2007.05905.x
- Genilloud, O. (2017). Actinomycetes: still a source of novel antibiotics. *Nat. Prod. Rep.* 34, 1203–1232. doi: 10.1039/C7NP00026J
- Giessen, T. W., Franke, K. B., Knappe, T. A., Kraas, F. I., Bosello, M., Xie, X., et al. (2012). Isolation, structure elucidation, and biosynthesis of an unusual hydroxamic acid ester-containing siderophore from *actinosynnema mirum*. *J. Nat. Prod.* 75, 905–914. doi: 10.1021/np300046k
- Heptinstall, S., Archibald, A. R., and Baddiley, J. (1970). Teichoic Acids and Membrane Function in *Bacteria*. *Nature* 225, 519–521. doi: 10.1038/225519a0
- Jones, L. J. F., Carballido-López, R., and Errington, J. (2001). Control of cell shape in *Bacteria*: helical, actin-like filaments in *Bacillus subtilis*. *Cell* 104, 913–922. doi: 10.1016/S0092-8674(01)00287-2
- Kawai, Y., Daniel, R. A., and Errington, J. (2009). Regulation of cell wall morphogenesis in *Bacillus subtilis* by recruitment of PBP1 to the MreB helix. *Mol. Microbiol.* 71, 1131–1144. doi: 10.1111/j.1365-2958.2009.06601.x
- Kishimoto, S., Nishimura, S., and Kakeya, H. (2015b). Total synthesis and structure revision of mirubactin, and its iron binding activity. *Chem. Lett.* 44, 1303–1305. doi: 10.1246/cl.150520
- Kishimoto, S., Nishimura, S., Hatano, M., Igarashi, M., and Kakeya, H. (2015a). Total synthesis and antimicrobial activity of chlorocatechelin A. *J. Org. Chem.* 80, 6076–6082. doi: 10.1021/acs.joc.5b00532
- Kishimoto, S., Nishimura, S., Hattori, A., Tsujimoto, M., Hatano, M., Igarashi, M., et al. (2014). Chlorocatechelins A and B from *Streptomyces* sp.: New siderophores containing chlorinated catecholate groups and an acylguanidine structure. *Org. Lett.* 16, 6108–6111. doi: 10.1021/ol502964s
- Koch, A. L. (2006). The exocytoskeleton. *Microb. Physiol.* 11, 115–125. doi: 10.1159/000094048
- Koo, B. M., Kritikos, G., Farelli, J. D., Todor, H., Tong, K., Kimsey, H., et al. (2017). Construction and analysis of two genome-scale deletion libraries for *Bacillus subtilis*. *Cell Syst.* 4, 291–305.e7. doi: 10.1016/j.cels.2016.12.013
- Koren, S., Walenz, B. P., Berlin, K., Miller, J. R., Bergman, N. H., and Phillippy, A. M. (2017). Canu: scalable and accurate long-read assembly via adaptive k-mer

## Publisher's note

All claims expressed in this article are solely those of the authors and do not necessarily represent those of their affiliated organizations, or those of the publisher, the editors and the reviewers. Any product that may be evaluated in this article, or claim that may be made by its manufacturer, is not guaranteed or endorsed by the publisher.

## Supplementary material

The Supplementary Material for this article can be found online at: <https://www.frontiersin.org/articles/10.3389/fmicb.2022.1004737/full#supplementary-material>

- weighting and repeat separation. *Genome Res.* 27, 722–736. doi: 10.1101/gr.215087.116
- Kritikos, G., Banzhaf, M., Herrera-Dominguez, L., Koumoutsis, A., Wartel, M., Zietek, M., et al. (2017). A tool named Iris for versatile high-throughput phenotyping in microorganisms. *Nat. Microbiol.* 2:17014. doi: 10.1038/nmicrobiol.2017.14
- Leaver, M., and Errington, J. (2005). Roles for MreC and MreD proteins in helical growth of the cylindrical cell wall in *Bacillus subtilis*. *Mol. Microbiol.* 57, 1196–1209. doi: 10.1111/j.1365-2958.2005.04736.x
- Lee, S., and Price, C. W. (1993). The minCD locus of *Bacillus subtilis* lacks the minE determinant that provides topological specificity to cell division. *Mol. Microbiol.* 7, 601–610. doi: 10.1111/j.1365-2958.1993.tb01151.x
- Levin, P. A., Margolis, P. S., Setlow, P., Losick, R., and Sun, D. (1992). Identification of *Bacillus subtilis* genes for septum placement and shape determination. *J. Bacteriol.* 174, 6717–6728. doi: 10.1128/jb.174.21.6717-6728.1992
- Masayuki, H., Seika, O., and Junichi, S. (2012). Synthetic lethality of the lytE cw10 genotype in *Bacillus subtilis* is caused by lack of d,l-endopeptidase activity at the lateral cell wall. *J. Bacteriol.* 194, 796–803. doi: 10.1128/JB.05569-11
- Meeske, A. J., Riley, E. P., Robins, W. P., Uehara, T., Mekalanos, J. J., Kahne, D., et al. (2016). SEDS proteins are a widespread family of *Bacterial* cell wall polymerases. *Nature* 537, 634–638. doi: 10.1038/nature19331
- Miethke, M., Klotz, O., Linne, U., May, J. J., Beckering, C. L., and Marahiel, M. A. (2006). Ferri-bacillibactin uptake and hydrolysis in *Bacillus subtilis*. *Mol. Microbiol.* 61, 1413–1427. doi: 10.1111/j.1365-2958.2006.05321.x
- Morath, S., Geyer, A., and Hartung, T. (2001). Structure–function relationship of cytokine induction by lipoteichoic acid from *Staphylococcus aureus*. *J. Exp. Med.* 193, 393–398. doi: 10.1084/jem.193.3.393
- Murray, T., Popham, D. L., and Setlow, P. (1998). *Bacillus subtilis* cells lacking penicillin-binding protein 1 require increased levels of divalent cations for growth. *J. Bacteriol.* 180, 4555–4563. doi: 10.1128/JB.180.17.4555-4563.1998
- Oku, Y., Kurokawa, K., Matsuo, M., Yamada, S., Lee, B. L., and Sekimizu, K. (2009). Pleiotropic roles of polyglycerolphosphate synthase of lipoteichoic acid in growth of *Staphylococcus aureus* cells. *J. Bacteriol.* 191, 141–151. doi: 10.1128/JB.01221-08
- Pedreira, T., Efmann, C., and Stülke, J. (2022). The current state of SubtiWiki, the database for the model organism *Bacillus subtilis*. *Nucleic Acids Res.* 50:D875–D882. doi: 10.1093/nar/gkab943
- Peuckert, F., Ramos-Vega, A. L., Miethke, M., Schwörer, C. J., Albrecht, A. G., Oberthür, M., et al. (2011). The Siderophore binding protein FeuA shows limited promiscuity toward exogenous triscatecholates. *Chem. Biol.* 18, 907–919. doi: 10.1016/j.chembiol.2011.05.006
- Pi, H., Wendel, B., and Helmann, J. (2022). Dysregulation of magnesium transport protects *Bacillus subtilis* against manganese and cobalt intoxication. *J. Bacteriol.* 202:e711–e719. doi: 10.1128/JB.00711-19
- Pu, H., Jiang, T., Peng, D., Xia, J., Gao, J., Wang, Y., et al. (2022). Degradation of mirubactin to multiple siderophores with varying Fe(III) chelation properties. *Org. Biomol. Chem.* 20, 5066–5070. doi: 10.1039/D2OB00942K
- Richter, S. G., Elli, D., Kim, H. K., Hendrickx, A. P., Sorg, J. A., Schneewind, O., et al. (2013). Small molecule inhibitor of lipoteichoic acid synthesis is an antibiotic for Gram-positive *Bacteria*. *Proc. Natl. Acad. Sci. U.S.A.* 110, 3531–3536. doi: 10.1073/pnas.1217337110
- Schirner, K., Marles-Wright, J., Lewis, R. J., and Errington, J. (2009). Distinct and essential morphogenic functions for wall- and lipo-teichoic acids in *Bacillus subtilis*. *EMBO J.* 28, 830–842. doi: 10.1038/emboj.2009.25
- Seemann, T. (2014). Prokka: rapid prokaryotic genome annotation. *Bioinformatics* 30, 2068–2069. doi: 10.1093/bioinformatics/btu153
- Tesson, B., Dajkovic, A., Keary, R., Marlière, C., Dupont-Gillain, C. C., and Carballido-López, R. (2022). Magnesium rescues the morphology of *Bacillus subtilis* mreB mutants through its inhibitory effect on peptidoglycan hydrolases. *Sci. Rep.* 12:1137. doi: 10.1038/s41598-021-04294-5
- Varley, A. W., and Stewart, G. C. (1992). The divIVB region of the *Bacillus subtilis* chromosome encodes homologs of *Escherichia coli* septum placement (minCD) and cell shape (mreBCD) determinants. *J. Bacteriol.* 174, 6729–6742. doi: 10.1128/jb.174.21.6729-6742.1992
- Vickery, C. R., Wood, B. M., Morris, H. G., Losick, R., and Walker, S. (2018). Reconstitution of *Staphylococcus aureus* lipoteichoic acid synthase activity identifies congo red as a selective inhibitor. *J. Am. Chem. Soc.* 140, 876–879. doi: 10.1021/jacs.7b11704
- Weidenmaier, C., Kokai-Kun, J. F., Kristian, S. A., Chanturiya, T., Kalbacher, H., Gross, M., et al. (2004). Role of teichoic acids in *Staphylococcus aureus* nasal colonization, a major risk factor in nosocomial infections. *Nat. Med.* 10, 243–245. doi: 10.1038/nm991
- Wilson, S., and Garner, E. (2021). An exhaustive multiple knockout approach to understanding cell wall hydrolase function in *Bacillus subtilis*. *bioRxiv* 2021.02.18.431929 [Preprint]. doi: 10.1101/2021.02.18.431929